Scientia Iranica B (2021) 28(5), 2613–2627

Sharif University of Technology
Scientia Iranica
Transactions B: Mechanical Engineering
http://scientiairanica.sharif.edu

Comprehensive evaluation of a semi-solar greenhouse: Energy, exergy, and economic analyses with experimental validation

B. Mohammadi[a], S.F. Ranjbar[a,*], and Y. Ajabshirchi[b]

a. *Department of Mechanical Engineering, Mechanical Engineering Faculty, University of Tabriz, Tabriz, Iran.*
b. *Department of Biosystems Engineering, Faculty of Agriculture, University of Tabriz, Tabriz, Iran.*

Received 16 June 2019; received in revised form 20 December 2020; accepted 17 May 2021

KEYWORDS
Dynamic model;
Semi-solar greenhouse;
Air unit cost;
Exergy destruction.

Abstract. This study conducts dynamic modeling and analysis of an innovative semi-solar greenhouse structure via MATLAB software in terms of energy, exergy, and economy. This modeling is used to predict the temperatures of four different area points inside a semi-solar greenhouse structure for the evapotranspiration of the crop. Measured data recorded from the constructed typical semi-solar greenhouse are used to evaluate the results of the proposed thermodynamic analysis. Measurements during the experiment show a considerable temperature difference of 20°C between the indoor and outdoor air. The mean values of 5.94% and 2.06°C for MAPE (Mean Absolute Percentage Error) and RMSE (Root Mean Squared Error) point to the accuracy of the thermal simulation. Furthermore, in different heat and mass transfer processes, the total exergy destruction values are analyzed. The target of this research is to provide suitable environmental conditions for the inside of the greenhouse. In this respect, the greenhouse air unit cost for each time step of one minute is inspected. By increasing the interest rate from 10% to 20%, the greenhouse air unit cost raises almost twice. Decrease of about 45.36% in total exergy destruction is obtained by the technique of applying double-layer glass as the greenhouse cover.

1. Introduction

Greenhouse cultivation is a popular intensive type of crop production with a yield per cultivated unit area more than 10 times larger than field crops. Heating and cooling of greenhouse are two of the most energy-consuming operations among the various activities performed for protected cultivation. The growing use of fossil fuels as an energy source has given rise to many side effects on the environment. In this respect, solar energy as an abundant, clean and sound source can be regarded as a favorable energy source rather than a conventional one. Solar energy with more suitable energy-saving properties can play a valuable role in greenhouse heating. Recently, researchers have performed many studies on the application of solar energy to greenhouse heating.

Utilizing mathematical modeling, Kiyan et al. [1] investigated the thermal behavior of a greenhouse heated by a hybrid solar collector system. They demonstrated the higher efficiency of coupling conventional fossil fuel-based systems with the proposed solar collectors despite their longer payback period. Gorjian et al. reviewed the development of solar greenhouses considering their coupling with solar en-

*. *Corresponding author.*
E-mail addresses: behzad6210@yahoo.com (B. Mohammadi); s.ranjbar@tabrizu.ac.ir (S.F. Ranjbar); yajabshir@tabrizu.ac.ir (Y. Ajabshirchi)

doi: 10.24200/sci.2021.53709.3375

ergy resources such as photovoltaic (PV), photovoltaic-thermal (PVT), and solar thermal collectors [2]. They concluded that solar thermal collectors installed in greenhouses in temperate climates exhibited higher efficiency. Kondili and Kaldellis [3] showcased an integrated geothermal-solar greenhouse and demonstrated that the proposed system could improve technical and economic efficiencies upon minimizing fossil fuel consumption. Energy, exergy, and economic analyses of different renewable resources integrated with PV systems were investigated recently by Li et al. and optimum state, exergy efficiency, and total cost rate of these systems were obtained [4–6]. Ziapour and Hashtroudi [7] carried out a simulation for a greenhouse with a curved glass roof equipped with a Phase Change Material (PCM) tubular collector to save the energy. Optimum values of 7.5 cm for the collector pipe radius and 17 lit for the PCM volume were obtained using an evolutionary algorithm. Sajid and Bicer made a cost comparison between four different systems supplied by solar energy to prepare electric energy, water, and air conditioning for a greenhouse system [8]. The minimum costs of electricity, cooling, and water were reported to be 0.033 \$/kWh, 0.015 \$/kWh, and 1.45 $\$/m^3$, respectively. Heating cost and the efficiency of the greenhouse could be enhanced using the potential of solar water collectors in the ground heat system during cold seasons [9]. Length of exchanger and the inlet flow rate were mentioned as effective elements on the performance of the proposed system. Heat cost reduction could go over 50% in April. Straw block north wall performance in solar greenhouses, thermal storage coefficient of storage layer, the total thermal inertia index, and the total thermal resistance of the storage wall as improved thermal characteristics were investigated by Zhang et al. [10]. They reported that the system had an efficient performance economically and environmentally. A combination of two heating systems, namely rock-bed thermal energy storage and water filled passive solar, was investigated in a study by Bazgaou et al. [11]. In this project, the use of the combined system covered the heating requirements of the greenhouse and the combination of two heating systems was very profitable which could generate profits for farmers. Joudi and Farhan [12] used a solar air heater to heat an innovative greenhouse structure in winter experimentally. They showed that 0.012 $kg/s/m^2$ of air mass flow rate could support almost 84% of the daily heat consumption. In addition, to maintain the greenhouse at a temperature of 18°C, the air mass flow rate through the collectors varied from 0.006 to 0.012 $kg/s.m^2$. Furthermore, to obtain more efficient and economical products, agricultural greenhouses are seek to apply maximum amounts of renewable energies. However, there are some meaningful distinctions between the ideal closed and traditional greenhouse layouts in terms of energy consumption and payback period [13]. Zhang et al. discussed a dynamic energy balance model considering dynamic cover absorbance and transmittance with an improved performance [14]. This study investigated the use of a sub-model of seven-layer soil and the solar radiation transmitted into the greenhouse from side walls. Moreover, the transmittance of various greenhouse surfaces, solar radiation absorbed by cover, and solar radiation transmitted into the greenhouse were investigated. Rapid calculation of physical dimensions of passive solar greenhouses was derived in a study by Chen et al. [15]. They demonstrated that this method was valid for a wide range of geographical latitudes. Zhang et al. designed passive heat-storage greenhouse walls for non-arable lands and established an unsteady model of the solar greenhouse's thermal environment [16]. They analyzed the thermal performances and energy efficiencies of these walls. The results verified the larger contributions of wall to promoting the thermal environment of solar greenhouses. A solar greenhouse integrated with Photovoltaic/Thermal (PV/T) and Earth-Air Heat Exchanger (EAHE) was thermally modeled by Mahdavi et al. [17]. Heating/cooling potential of PV/T and EAHE integration into greenhouse were studied. They recommended PV rather than PV/T integration while heating/cooling potential of EAHE was noticeable.

Application of PCM as fluid flow in ventilation proposed by Chen et al. [18] to inspect the effective elements. They illustrated that the north wall could save more energy and the crops could be yielded sooner upon using this methodology. Tomato cultivation was taken into account by Yildizhan and Taki [19] to obtain more effective products. They used the cumulative exergy approach in various regions of Turkey and reported some improvements in energy and exergy efficiencies.

Greenhouses have considerable capacities to save and use great quantities of solar energy in fruit and vegetable cultivation. Most greenhouses in developing countries, especially Iran, use fossil fuels due to the high frequency of oil and gas sources. Therefore, to our knowledge, previous studies have disregarded the energetic, exergetic, and economic evaluation of a semi-solar greenhouse under Iran's conditions up until now. In this research, simulating the heat and mass transfer in a semi-solar greenhouse by an innovative dynamic model and, then, inspecting the exergy destructions through processes were taken into account to compensate the lack of information in this field. Particularly, there are no noticeable inquiries on the experimental inspection of solar greenhouses. The final part of this study concentrates on the exergoeconomic assessments and offers some economic suggestions. Modeling results are validated based on the measured values from the

constructed greenhouse of 15 m^2. The results of this project can be used in commercialization of semi-solar greenhouses in the future, and they help farmers and customers decrease crop costs. The main innovations of this study can be stated as follows:

- Suggesting a dynamic model to predict the temperature and relative humidity of a semi-solar greenhouse;
- Using statistical functions to define the precision of the modeling;
- Evaluating the dynamic model conclusions using the data obtained from experiments;
- Exergoeconomic investigation of the semi-solar greenhouse.

2. Materials and methods

2.1. Semi-solar greenhouse

For experimental evaluation of the thermodynamic simulation in this study, an innovative structure was designed and installed in Tabriz city, Azerbaijan Province, Iran (Latitude 38° 100′N). Researchers demonstrated that greenhouse heating consumed over than 30% of its total operational energy [18]. Furthermore, to harness the highest amount of solar energy in greenhouse structures, the shape and orientation of a greenhouse are highly emphasized [20]. Then, attempting to select the most suitable shape and orientation for the constructed structure, the present study inspects many shapes from the viewpoint of solar energy capture in two main orientations of east-west and north-south. In this way, the greenhouse structure and orientation are chosen upon radiation calculation and based on Tabriz Meteorological Information Center [21] (Figure 1).

The selected structure is called "semi-solar" because of its well-suited structure in absorbing solar radiation and using thermal screen and block north wall to save solar energy and avoid energy loss.

A semi-solar greenhouse was constructed by glass covering on a land with 5 m length and 3 m width. Data recording was performed in this greenhouse by cabbage as an experiment specimen to validate the results of thermal simulation. The considered assumptions are as follows:

- The sole ventilation is the windows leakage;
- Evapotranspiration is considered;
- All greenhouse elements have a constant temperature;
- The surface evaporation of the greenhouse land is not considered;
- CO_2 variation impact is ignored.

2.2. Internal and external climate data

The experiment began since 9:00 a.m. and lasted for 8 hours with cabbage cultivation on 28 November, 2017. There was not any rain or snow along the data recording. Temperature and relative humidity of greenhouse components were measured by a 14-bit analog to digital sensors. By increasing the accuracy of the recorded data, two sensors were taken into account for every component and the mean of the two measured data was considered in calculations. Solar radiation absorbed by greenhouse components was assessed by TES1333 sensors installed on the roof and surface of plant and soil with sensibility of 5% W/m^2. Outside air velocity was gauged by ST8894 anemometer and all obtained data were recorded by a 16-bit resolution data recorder with 5000 measurements per second power. Location of temperature and relative humidity sensors installed in the greenhouse are given in Figure 2.

2.3. Performance evaluation criteria

Uncertainty analysis was employed to evaluate the preciseness of data recording. Accordingly, the experi-

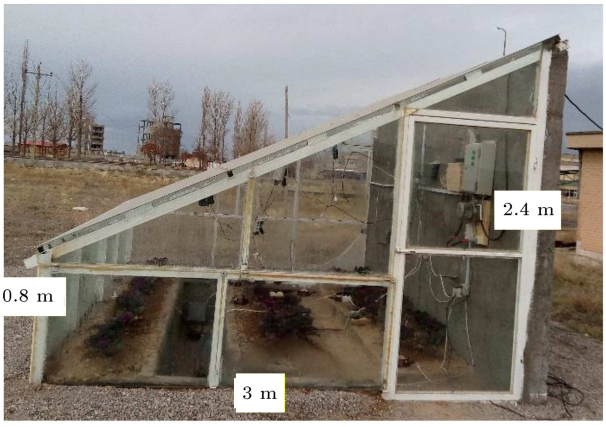

Figure 1. Selected greenhouse structure for the present study.

Figure 2. Location of temperature and relative humidity sensors installed at the greenhouse.

ments were done all over again on November 29 and 30, 2017 with the same conditions of the main experiment and the obtained data from consecutive days were assessed with uncertainty analysis. The mean of the gauged data is obtained as follows [22]:

$$\overline{X} = \frac{\sum X_m}{n}. \tag{1}$$

Let n be the measurement series and X_m the gauged value. Standard deviation is calculated as in the following [22]:

$$SD = \sqrt{\frac{\sum_{m=1}^{n} \left(X_m - \overline{X}\right)^2}{(n-1)}}. \tag{2}$$

Then, uncertainty is obtained as follows [22]:

$$U = \frac{SD}{\sqrt{n}}. \tag{3}$$

Furthermore, two statistical functions of Mean Absolute Percentage Error (MAPE) and Root Mean Squared Error (RMSE) were employed to assess the accuracy of the thermal modeling [23]:

$$MAPE = \frac{1}{n}\sum_{j=1}^{n}\left|\frac{d_j - p_j}{d_j}\right| \times 100, \tag{4}$$

$$RMSE = \sqrt{\frac{\sum_{j=1}^{n}(d_j - p_j)^2}{n}}. \tag{5}$$

2.4. Modeling and analysis

Energy flows and exergy destruction procedure are presented in Figure 3. Significant heat transfers by long/short wave radiation, convection, and conduction were assessed. In addition, some important mass transfers by air and vapor were discussed. Then, a comprehensive evaluation of a semi-solar greenhouse including energy, exergy, and economic analyses was conducted by simulating the enthalpy balance equations in MATLAB software in equal time steps. The results were validated by the measured values during the experiment on November 28, 2017. Flowchart of the developed dynamic model is illustrated in Figure 4.

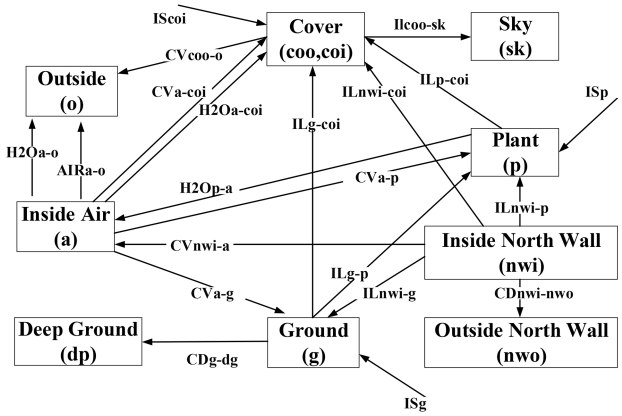

Figure 3. Schematic of significant heat/mass transfers by long/short wave radiation, convection, conduction, air, and vapor.

Table 1 represents the input parameter values used for thermodynamic simulation.

2.4.1. Energy view

Eqs. (6)–(9) as shown in Box I are used to calculate the temperature variations of inside air (T_a), inside ground (T_g), plant (T_p), and inside cover (T_{coi}) in each time step [23,26,27]. Tables 2, 3, 4, and 5 show heat transfer between greenhouse components by convection, conduction, and long-wave and short-wave radiations, respectively. In addition, Tables 6 and 7 list the heat transfer between greenhouse components by mass transfer of air and H_2O, respectively.

In the building industry, two-layer glass windows are sometimes applied to reduce energy loss by convection heat transfer due to temperature difference

$$\frac{dT_a}{dt} = \frac{Q_{a-g} - Q_{a-p} - Q_{a-coi} - Q_{nwi-nwo}}{\rho_a \times c_{p-a} \times V_a}, \tag{6}$$

$$\frac{dT_g}{dt} = \frac{Q_{rd-g} - Q_{a-g} - Q_{g-p} - Q_{g-coi} - Q_{g-dg}}{(0.7 \times \rho_g \times c_{p-g} + 0.2 \times \rho_{\mathrm{H_2O}} \times c_{p-\mathrm{H_2O}} + 0.1 \times \rho_a \times c_{p-a}) \times V_g}, \tag{7}$$

$$\frac{dT_p}{dt} = \frac{Q_{rd-p} + Q_{a-p} + Q_{coi-p} + Q_{g-p} - Q_{\mathrm{H_2O}}, p-a}{\rho_p \times c_{p-p} \times V_p}, \tag{8}$$

$$\frac{dT_{coi}}{dt} = \frac{Q_{rd-coi} + Q_{a-coi} + Q_{\mathrm{H_2O}}, a-coi + Q_{g-coi} - Q_{coi-p} - Q_{coo-o} - Q_{coo-\mathrm{sky}}}{\rho_{coi} \times c_{p-coi} \times V_{coi}}. \tag{9}$$

Box I

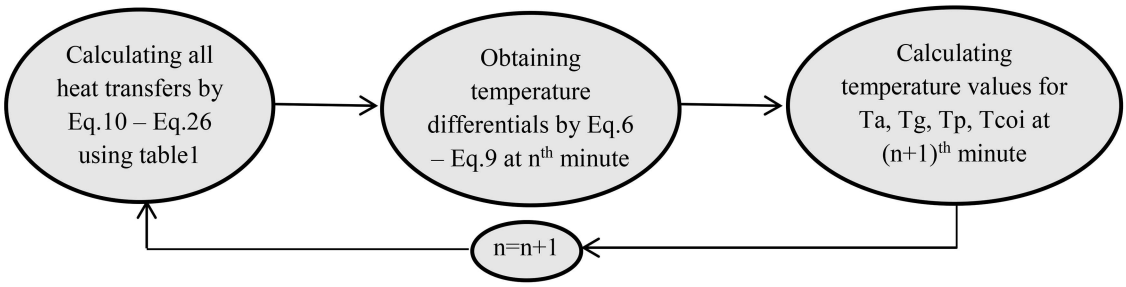

Figure 4. Flowchart of the developed dynamic model.

Table 1. Input parameter values [24–27].

Parameter	Value	Parameter	Value	Parameter	Value
A_g	15	E_{coi}	0.95	l_f	0.004
A_p	15	E_{coo}	0.95	$R_{\min}$	82.003
A_{sc}	15	E_{nw}	0.7	V_a	24
A_{coi}	17	E_{sk}	0.8	V_g	9.75
A_{coo}	17	F_{g-p}	0.472	V_{sc}	0.03
$c_{p,a}$	1000	$F_{g\text{-}sc}$	0.528	V_{co}	0.06
$c_{p,\mathrm{H_2O}}$	4186	F_{g-coi}	0.8	v_a	0.09
$c_{p,sc}$	1500	$F_{g\text{-}nwi}$	0.528	η_{vhr}	0.9
$c_{p,g}$	800	$F_{p\text{-}sc}$	0.472	$\eta_{rd,coi}$	0.017
$c_{p,coi}$	840	$F_{p\text{-}nwi}$	0.472	$\eta_{rd,g}$	0.331
$c_{p,coo}$	840	$F_{p\text{-}coi}$	0.528	$\eta_{rd,p}$	0.258
d_{co}	0.004	$F_{sc\text{-}nwi}$	0.528	σ	5.67051×10^{-8}
d_g	0.65	$F_{sc\text{-}coi}$	1	r_w	2.26×10^6
d_{sc}	0.002	$F_{nwi\text{-}coi}$	0.528	ρ_a	$1.29\frac{T_a}{T_0}$
d_{nw}	0.25	$F_{coo\text{-}sk}$	0.86	ρ_g	1400
E_g	0.7	f_a	1	ρ_{co}	2500
E_p	0.472	LAI	1.04	ρ_{sc}	2000
E_{sc}	0.9	Le (Lewis number)	0.89		

between the glass surface and inside/outside air. These two-layer glass windows are usually manufactured from glass with thickness of 4 mm with a vacuumed or a gas-filled space. In this research, a standard type of two-layer glass (with convection heat transfer coefficient of 0.35 $\frac{\mathrm{W}}{\mathrm{m^2\ K}}$) was applied as a greenhouse cover, and its effect on the energy saving and exergy destruction reduction was calculated [24,25].

2.4.2. Exergy view

The maximum work presented through enthalpy transfer between a system and its surroundings is defined as exergy while moving in the direction of balance with its environment [30]. Exergy destruction through enthalpy transfer between systems A and B by convection, conduction, and long wave radiation heat transfers is described as follows [31]:

$$EX_d = -QT_e\left(\frac{1}{T_B} - \frac{1}{T_A}\right). \tag{10}$$

Let Q, T_e, T_A, and T_B be the heat transferred from T_A to T_B, environment temperature, and systems of A and B temperatures, respectively.

Furthermore, exergy destruction through mass transfer between systems A and B by air through ventilation or leakage is calculated by Eq. (27).

Exergy destruction by enthalpy transfer through vapor dewing below the interior side of the cover is described as [31]:

$$EX_d = -n_i RT_e \ln\left(\frac{p_{i,A}}{p_{i,B}}\right). \tag{11}$$

Let n_i, $p_{i,A}$, and $p_{i,B}$ represent the quantity of species i as well as the partial pressure of species A and B, respectively. In addition, exergy destruction through transpiration of crop is calculated using Eq. (28).

In the test, it is considered that all windows and doors are plugged and the sole ventilation is the windows leakage. Then, the exergy destruction through vapor transfer through leakages between inside and outside is described as follows [31]:

Table 2. Heat transfer between greenhouse components by convection [26].

Heat transfer between inside air and plant:	
$Q_{a-p} = A_{a-p} \times \alpha_{a-p}(T_a - T_p)$	Eq. (23)
$\alpha_{a-p} = \frac{\rho_a \times c_{p-a}}{R_{b-\text{heat}}}$	
$R_{b-\text{H2O}} = \frac{1174\sqrt{l_f}}{(l_f \times \lvert T_p - T_a \rvert + 207 v_a^2)^{1/4}}$	
$A_{\alpha-p} = 2 \times LAI \times A_g$	
$LAI = \frac{\text{Total leaves area}}{\text{Greenhause land area}}$ (In this study, LAI (Leaf Area Index) was measured 1.04)	
$A_{\alpha-g} = 15\ \text{m}^2$	
Heat transfer between inside air and ground:	
$Q_{a-g} = A_{a-g} \times \alpha_{a-g}(T_a - T_g)$	Eq. (24)
$\alpha_{a-g} = 1.3 \times \lvert T_a - T_g \rvert^{0.25}$ $\quad T_a \geq T_g$	
$\alpha_{a-g} = 1.7 \times \lvert T_a - T_g \rvert^{0.33}$ $\quad T_a \leq T_g$	
Heat transfer between inside air and inside cover:	
$Q_{a-g} = A_{a-coi} \times \alpha_{a-coi}(T_a - T_{coi})$	Eq. (25)
$\alpha_{a-coi} = 3 \times \lvert T_a - T_{coi} \rvert^{1/3}$	
$A_{a-coi} = 17.7\ \text{m}^2$	
Heat transfer between outside air and outside cover:	
$Q_{coo-o} = A_{coo-o} \times \alpha_{coo-o}(T_{coo} - T_o)$	Eq. (26)
$\alpha_{coo-o} = 2.8 + 1.2 v_0$ $\quad v_0 \prec 4$	
$\alpha_{coo-o} = 2.8 v_0^{0.8}$ $\quad v_0 \geq 4$	
$A_{a-coi} = 17.7\ \text{m}^2$	

Table 3. Heat transfer between greenhouse components by conduction [26].

Heat transfer between inside wall and outside wall:	
$Q_{nwi-nwo} = A_{nw} \times (\lambda_{nw}/d_{nw})(T_{nwi} - T_{nwo})$	Eq. (27)
$\lambda_{nw} = 0.0625\ \frac{\text{w}}{\text{mK}}$	
$d_{nw} = 0.25\ \text{m}$	
$A_{nw} = 11.52\ \text{m}^2$	
Heat transfer between ground and deep grounds:	
$Q_{g-dg} = A_d \times (\lambda_g/d_g)(T_g - T_{dg})$	Eq. (28)
$\lambda_g = 0.6710\ \frac{\text{w}}{\text{mK}}$	
$d_g = 0.4208\ \text{m}$	
$A_{nw} = 15\ \text{m}^2$	

$$EX_d = -RT_e(n_{i,A} - n_{i,B}) \ln\left(\frac{p_{i,A}}{p_{i,B}}\right). \quad (12)$$

The inside air exergy is calculated by the concept of wet air in air-conditioning systems. The air of inside greenhouse is supposed to be a combination of vapor and dry air so that its total exergy can be obtained by calculating the exergy of vapor and dry air separately. Then, the inside air exergy is achieved by computing the thermal and diffusional exergy of the air in one minute time steps by the equations listed in Tables 8 and 9 [32]. Environment temperature (T_e) and pressure (P_e) are supposed to be the reference conditions [31].

In the exergy analysis of the greenhouses, the outside air reference conditions have an insignificant impact [31].

2.4.3. Economic view

An efficient procedure is employed to obtain maximum efficiency and productivity with the lowest expense. In this way, some common social, economic, and technical issues should be taken into account. Economic evaluation of a system from the exergy viewpoint facilitates inspecting the cost of irreversibilities. In fact, the assessment of the component exergy destruction values by their expenses in a procedure can suggest a trustworthy method for improving its real efficiency [33].

Table 4. Heat transfer between greenhouse components by long wave radiation [26,27].

Heat transfer between ground air and plant:	
$Q_{g-p} = A_g \times E_g \times E_p \times F_{g-p} \times \sigma(T_g^4 - T_p^4)$	Eq. (29)
$F_{g-p} = 1 - \tau_{p-Il}$	
$E_{g-p} = 1 - \tau_{p-Il}$	
$\tau_{p-Il} = e^{-\kappa_{p-I} \times LAI}$	
$\kappa_{p-I} = 0.64$	
$E_g = 0.7$	
$\sigma = 5.67051 \times 10^{-8}$	
Heat transfer between ground and inside cover:	
$Q_{g-coi} = A_g \times E_g \times E_{coi} \times F_{g-coi} \times \sigma(T_g^4 - T_{coi}^4)$	Eq. (30)
$F_{g-coi} = 1 - F_{g-p}$	
$E_{coi} = 0.95$	
Heat transfer between inside cover and plant:	
$Q_{coi-p} = A_{coi} \times E_{coi} \times E_p \times F_{coi\text{-}p} \times \sigma(T_{coi}^4 - T_p^4)$	Eq. (31)
$F_{coi-p} = F_{coi-\text{sky}}(1 - \tau_{c-Il})$	
$F_{coi-\text{sky}} = \frac{A_g}{A_{coi}}$	
$A_{coi} = 17.7\ \text{m}^2$	
Heat transfer between outside cover and sky:	
$Q_{coo-\text{sky}} = A_{coo} \times E_{coo} \times E_{\text{sky}} \times F_{coo-\text{sky}} \times \sigma(T_{coo}^4 - T_{\text{sky}}^4)$	Eq. (32)
$E_{coo} = E_{coi}$	
$E_{\text{sky}} = 0.8$	
$A_{coo} = 17.7\ \text{m}^2$	
$T_{\text{sky}} = 0.0552(T_0)^{1.5}$	

Table 5. Heat absorbed by greenhouse components through short wave radiation [26,27].

Heat absorbed by ground:	
$Q_{rd,g} = A_g \times \eta_{rd,g} \times I_{\text{in}}$	Eq. (33)
$\eta_{rd,g} = 0.0028\tau_{p-Il} + 0.0045$	
I_{in} was measured by installed sensors	
Heat absorbed by plant:	
$Q_{rd,p} = A_p \times \eta_{rd,p} \times I_{\text{in}}$	Eq. (34)
$\eta_{rd,p} = 0.0089 - 0.0239\beta_{g-Is}$	
$\beta_{g-Is} = 0.58$	
Heat absorbed by inside cover:	
$Q_{rd,coi} = A_{coi} \times \eta_{rd,coi} \times I_{\text{in}}$	Eq. (35)
$\eta_{rd,coi} = 0.02\sqrt{\tau_{coi-Is}}$	
$\tau_{coi-Is} = 0.75$	

Table 6. Heat transfer between greenhouse components by air transfer [27–29].

$Q_{a-o} = (1 - op_{vhr} \times \eta_{vhr}) \times \rho_a \times c_{p-a} \times \phi_{\text{leak},a-o}(T_a - T_o)$	Eq. (36)
$\eta_{vhr} = 0.9$	
op_{vhr}	
$\phi_{\text{leak},a-o} = A_s(8.3 \times 10^{-5} + 3.5 \times 10^{-5} v_0 \times f_a)$	
f_a	
Infiltration factor (f_a) for the new greenhouse is one [29].	
$\eta_{vhr} = 0.9$	
op_{vhr} (Option ventilation heat recovery) is 1 or 0.	

Table 7. Heat transfer between greenhouse components by H_2O transfer [27–29].

Heat transfer between plant and inside air:

$$Q_{H_2O,p-a} = r_w \times \phi_{mH_2O,p-a} \quad \text{Eq. (37)}$$

$$\phi_{mH_2O,p-a} = \max\{A_p \times \kappa_{H_2O,p-a}(C_{H_2Os,p} - C_{H_2O,a}), 0\}$$

$$\kappa_{H_2O,p-a} = \frac{1}{R_{b-H_2O} + \frac{R_{cut} \times R_{s-H_2O}}{R_{cut} + R_{s-H_2O}}}$$

$$R_{cut} = 2000$$

$$R_{s-H_2O} = R_{min} \times f_l \times f_{TC} \times f_{CO2} \times f_{H_2O}$$

f_{CO_2}, f_I, f_{Tc}, and f_{H_2O}. represent CO_2 dependency, radiation dependency, temperature dependency, and H_2O dependency, respectively. These factors are defined in Table 8.

$$r_w = 2.26 \times 10^6 \ \frac{J}{kg}$$

$$C_{H_2Os,p} = \frac{P_{H_2Os.p} \times M_{H_2O}}{R_g \times T_p}$$

$$C_{H_2O,a} = (RH_a \times C_{a-H_2Os})/100$$

$$P_{p-H_2Os} = 610.780e^{\frac{17.08085(T_p - T_0)}{234.175 + (T_p - T_0)}}$$

$$M_{H_2O} = 18 \times 10^{-3} \ \frac{kg}{mol}$$

$$R_g = 8.314 \ \frac{kg}{mol.K}$$

$$T_0 = 273.15 \text{ K}$$

$C_{H_2O,a}$ was measured by installed sensors.

Heat transfer between inside cover and inside air:

$$Q_{H_2O,a-coi} = r_w \times \phi_{mH_2O,a-coi} \quad \text{Eq. (38)}$$

$$\phi_{mH_2O,a-coi} = \max\{A_{coi} \times \kappa_{H_2O,a-coi}(C_{H_2Os,coi} - C_{H_2O,a}), 0\}$$

$$\kappa_{H_2O,a-coi} = \frac{\alpha_{a-coi}}{\rho_a \times c_{p-a} \times Le^{2/3}}$$

$$\alpha_{a-coi} = 3 \times |T_a - T_{coi}|^{1/2}$$

$$C_{H_2Os,a} = \frac{P_{H_2Os.a} \times M_{H_2O}}{R_g \times T_a}$$

$$C_{H_2O,a} = (RH_a \times C_{a-H_2Os})/100$$

$$P_{coi-H_2Os} = 610.780e^{\frac{17.08085(T_{coi} - T_0)}{234.175 + (T_{coi} - T_0)}}$$

Heat transfer between inside air and outside:

$$Q_{H_2O,a-o} = r_w \times \phi_{mH_2O,a-o} \quad \text{Eq. (39)}$$

$$\text{Original cost} = \frac{\text{Cost index for the year when the original cost was obtained}}{\text{Cost index for the reference year}} \times \text{Cost at reference year.} \quad (13)$$

Box II

For economic evaluation of the greenhouse, the subsequent assumptions are regarded as follows:

- It is assumed that the semi-solar greenhouse is used contiguously;
- The lifetime of greenhouse components is considered to be ten years excluding the cover;
- The greenhouse cover lifetime is five years;
- The salvage cost of the greenhouse components is regarded 40% of the capital investment [20].

In this research, the 2012 reference cost data were applied to analyze the components of the semi-solar greenhouse system economically. Table 10 shows the details of greenhouse expenses according to the 2012 reference cost data [34].

Eq. (13) shown in Box II, converts the greenhouse expenses in the reference year to the present time [33].

In this research, the Marshall and Swift equipment cost index [35] was applied to be used in the above formulation as cost index. Therefore, for the reference year (2012) and the spring of 2019, the indices of 1889.4 and 2725.4 were applied, respectively.

Expense rate per time unit for each part of the

Table 8. Formulation of dependency factors for stomata resistance calculation.

f_{CO_2}	1
f_l	$\frac{\frac{I_{p-g}}{2LAI}+4.3}{\frac{I_{p-g}}{2LAI}+0.54}$ $[I_{p-g}=(0.0089-0.023\beta_{g-Is})I_{\text{in}}\beta_{g-Is}=0.58]$
f_{TC}	$1+0.005(T_p-T_0-33.6)^2$ $T_0=273.15$
f_{H_2O}	$\frac{4}{\sqrt[4]{1+255e^{-0.5427\Delta_{pp-H_2Om}}}}$ $\Delta_{pp-H_2Om}=0.01(p_{p-H_2Os}-p_{a-H_2O})]$

Table 9. Formulation of calculating the exergy of the greenhouse inside air.

$EX_{a,th}=c_p^*(T_a-T_0)-T_0(c_p^*\log\left(\frac{T_a}{T_0}\right)-R^*\log\left(\frac{p_a}{p_0}\right)$
$EX_{a,\text{dif}}=T_0\left[R^*\log\left(\frac{1+Y\omega_0}{1+Y\omega}\right)+CR_a\omega\log\left(\frac{\omega}{\omega_0}\right)\right]$
$c_p^*=c_{p-a}+\omega.c_{p-v}$
$R^*=R_a+\omega.R_v$
$Y=\frac{M_{\text{air}}}{M_{H_2O}}$
$\omega=0.622\left(\frac{p_{H_2O,a}}{p_a-p_{H_2O,a}}\right)$

Table 10. The greenhouse expenses details according to the 2012 reference cost data.

Parts	Reference expense ($)
Building	5340
Supporting supplies	
Measuring tools	1330
Heating system	420
Others	170
Workforce	1800
Experiment specimen	90
Electrical heating	0
Sum	9150

greenhouse is obtained as follows [36]:

$$\dot{Z}_k = CRF \times \frac{\phi_r}{N \times 3600} \times Z_k. \tag{14}$$

Let N be the number of hours that the system is used, Z_k the expense of the greenhouse parts, $\Phi_r = 1.06$ the maintenance factor, and CRF the Capital Recovery Factor:

$$CRF = \frac{i(1+i)^n}{(1+i)^n - 1}. \tag{15}$$

Let i be the interest rate and n the lifetime of each greenhouse part in years.

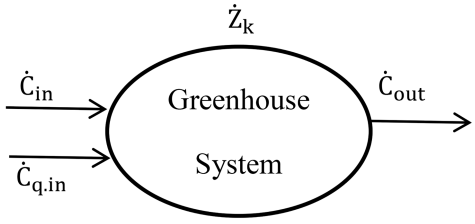

Figure 5. The flowchart of the cost flow in the greenhouse as a control mass for every time step.

The flowchart of the cost flow in the greenhouse as a control mass is shown in Figure 5 for every time step.

The following equation describes the cost balance in the greenhouse system:

$$\dot{C}_n + \dot{C}_{q,\text{in}} + \dot{Z}_k = \dot{C}_{\text{out}}. \tag{16}$$

In this equation, the sum of inlet cost rate (related to wet air), capital investment rate, and non-solar energy cost rate should be taken into account by obtaining the outlet cost rate of wet air. During the test, no non-solar energy source is employed and, then, non-solar energy cost rate ($\dot{C}_{q,\text{in}}$) is zero.

Upon applying Eq. (33) for every time step, we have the following:

$$\dot{C}_{n,\text{in}} + \dot{Z}_k = \dot{C}_{n,\text{out}}. \tag{17}$$

In addition, the outlet cost rate of the nth step could be regarded as the inlet cost rate of the $(n+1)$th step as follows:

$$\dot{C}_{n,\text{in}} + \dot{Z}_k = \dot{C}_{n+1,\text{in}}. \tag{18}$$

Considering that this research has the objective of providing suitable environmental conditions for the inside of the greenhouse, Eq. (19) is described in the following by canceling the time parameter:

$$C_{n,\text{in}} + Z_{k,n} = C_{n+1,\text{in}}, \tag{19}$$

where $C_{n,\text{in}}$ and $C_{n+1,\text{in}}$ represent the inlet cost of inside air related to the nth and $(n+1)$th time steps, respectively, and $Z_{k,n}$ is the capital investment of one time step (one minute) described as follows:

$$Z_{k,n} = 60 \times \dot{Z}_k. \tag{20}$$

Because of using the outside air as the primary inlet air of the greenhouse, the inlet cost of inside air related to the first time step is zero ($C_{1,\text{in}}$); thus, we have:

$$Z_{k,1} = C_{2,\text{in}}. \tag{21}$$

Applying the inside air exergy discussed in Subsection 2.4.2, the air unit cost of every time step is defined as follows:

$$c_{n+1,\text{in}} = \frac{c_{n.\text{in}} + 60\dot{Z}_k}{EX_{n+1}}. \tag{22}$$

3. Results and discussion

3.1. Energy and Exergy analysis results

The performance of the dynamic model and the innovative semi-solar greenhouse structure is studied in energetic and exergetic terms. Figure 6 presents variations in the experimental temperatures of the greenhouse parts (constructed in Tabriz city) and the outside air since 9:00 for 8 hours. The data was recorded every one minute.

In this experimental set, the inside cover was manufactured from a single-layer glass; then, its inside and outside surfaces had a few temperature differences. Therefore, the inside surface of the cover had a significant temperature difference from the inside air, leading a considerable amount of energy loss. Therefore, energy efficiency was reduced because of normal heat transfers by radiation and convection from the cold surface of the greenhouse cover and other greenhouse parts.

Based on Figure 6, the average temperature of the greenhouse air during the test was 33°C, almost 20°C more than the outside air temperature; then, the installed structure could prepare an acceptable situation for crop cultivation in cold days, because its performance in absorbing and keeping the solar energy during the test was efficient and comparable to those in other researches [37–43]. Uncertainty assessment results are listed in Table 11. As discussed before, the experiments were done all over again on November 29 and 30, 2017 with the same conditions as the main experiment on November 28, 2017 and the data obtained from consecutive days were evaluated using uncertainty analysis. The results indicated that the experimental measurements during the tests were reliable to evaluate the accuracy of the thermodynamic modeling.

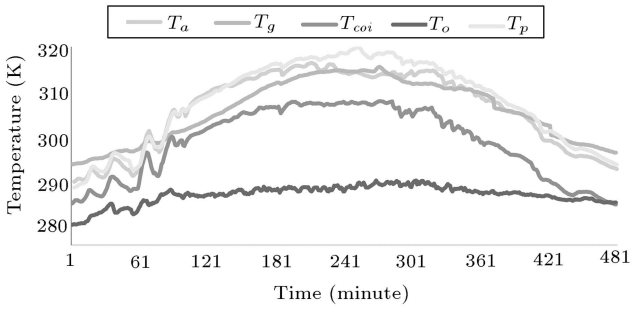

Figure 6. Changes in the experimental temperatures of the greenhouse parts and the outside air.

Table 11. The uncertainty analysis results.

Measurement devices	Uncertainty (U)
SHT11 (T_p)	±0.387 K
SHT11 (T_{coi})	±0.311 K
SHT11 (T_a)	±0.243 K
SHT11 (T_g)	±0.425 K
SHT11 (RH_a)	±0.263 RH
SHT11 (RH_o)	±0.314 RH
ST8894 (v_o)	±0.098 m/s
TES1333 (I_{in})	±1.23 $\frac{\text{W}}{\text{m}^2}$

Thermodynamic simulation of the semi-solar greenhouse was done using an innovative dynamic model by MATLAB software. Figure 7 compares the thermal modeling results with the experimental data recorded from the constructed greenhouse.

Figure 7 shows that thermal modeling results have an acceptable concurrence with the experimental data recorded from constructed greenhouse. In this respect, two statistical functions of MAPE and RMSE were employed to assess the accuracy of the thermal modeling, as given in Table 12.

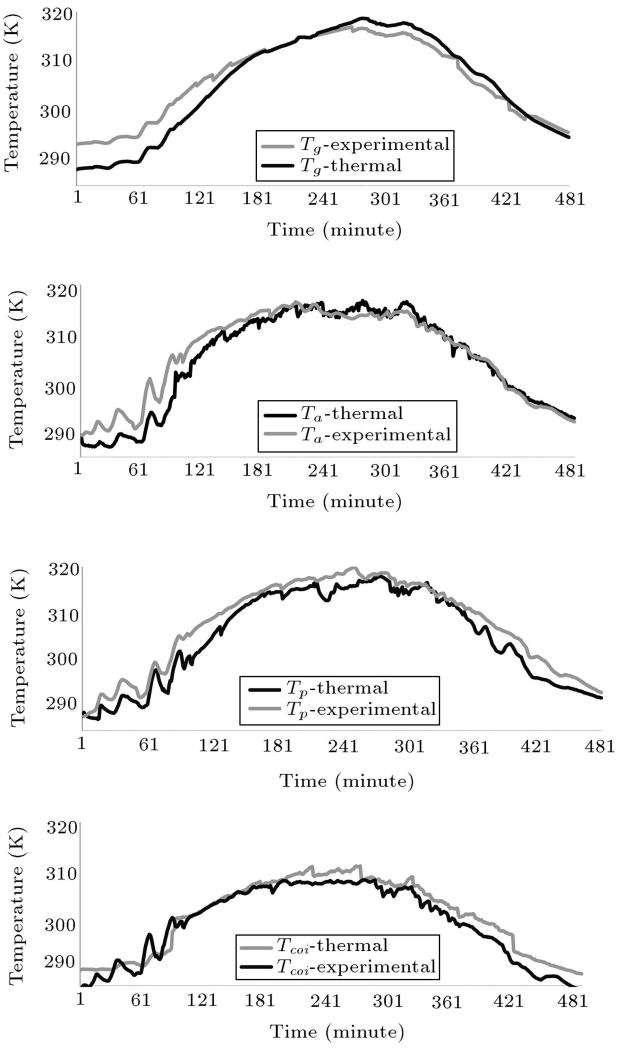

Figure 7. Thermal modeling results and experimental data recorded from the constructed greenhouse.

Table 12. Statistical evaluation results.

Temperature	MAPE (%)	RMSE (°C)
T_p	6.76	2.41
T_{coi}	5.42	1.89
T_a	5.11	2.18
T_g	6.47	1.75

In a theoretical study on a solar greenhouse [44], simulation results of inside air temperature and relative humidity and canopy temperature were compared with the experimental data recorded in 2007, and the range of 1.3°C to 2.36°C was obtained for RMSE. In other research studies [45,46], absolute errors of 10% and 20% were calculated between the modeling results and experimental measurements of the inside air temperature of the greenhouse.

According to the three discussed studies [44–46] and the statistical analysis results presented in Table 12, it can be deduced that the applied thermal simulation is credible.

Figure 8 represents the total exergy destruction values in different heat and mass transfer processes. This figure shows that the total exergy destruction associated with convection processes has the highest level among other heat transfer methods. This happens due to the considerable difference between the temperature of greenhouse cover and that of the inside and outside air. Hence, decreasing this temperature difference has a significant impact on reducing the total exergy destruction associated with convection processes ($EX_{d,CV,coo-o}$ and $EX_{d,CV,coi-a}$). Accordingly, a standard type of two-layer glass (with convection heat transfer coefficient of 0.35 W/m^2 K) was applied as a

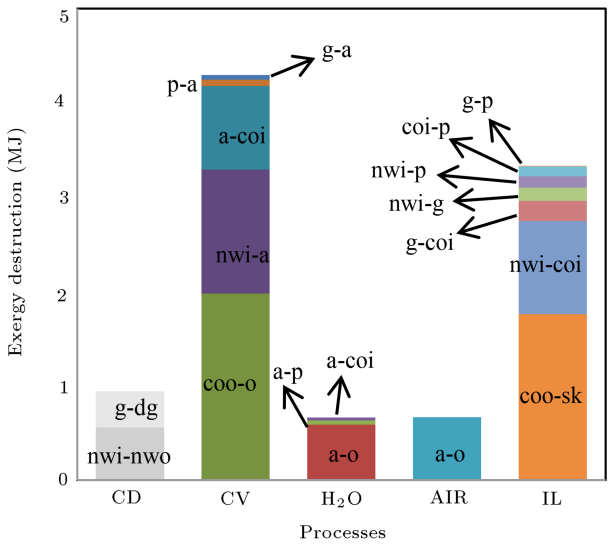

Figure 8. Exergy destruction values in different heat and mass transfer processes.

Table 13. Double layer glass impacts on the exergy destructions associated with different processes.

Processes	Exergy destruction value
$EX_{d,coo-o}$	49%
$EX_{d,a-coi}$	48.5%
$EX_{d,coo-sk}$	46.2%
$EX_{d,nwi-coi}$	36.3%
$EX_{d,g-coi}$	31.5%
$EX_{d,p-coi}$	29.4%

greenhouse cover to reduce the energy loss and exergy destruction. Comparison of the performance of double-layer glass separated with the air-filled space and that of one-layer glass as greenhouse cover was made using a dynamic model. A reduction of 49% in $EX_{d,CV,coo-o}$ value was detected due to diminishing the temperature difference between the greenhouse cover and outside air.

Furthermore, double-layer glass application results showed a considerable decrease in the exergy destruction associated with convection heat transfer between the greenhouse cover and interior air ($EX_{d,CV,coo-o}$); similarly, the exergy destruction is related to heat transfer between cover and sky by radiation ($EX_{d,IL,coo-sk}$). Using double-layer glass as a greenhouse cover facilitated a condition in which the interior surface of the cover was maintained at high temperatures while the outside surface of the cover was exposed to low temperatures. Double-layer glass impacts on the exergy destructions associated with different processes are listed in Table 13.

Exergy loss due to the air flow from the inside to the outside of the greenhouse takes place in two forms: exergy flow by dry air and exergy flow by vapor [22]. This air flow occurs because of the leakages in windows and doors. Then, the exergy losses can be reduced calking windows and doors. Eventually, the exergy destruction associated with the condensation of vapor on the inside surface of the greenhouse cover and respiration of the crop were very low and insignificant.

3.2. Economic analysis results

The air unit cost of the semi-solar greenhouse is presented in Figure 9 and is measured using Eq. (39) for three interest rates since minute 1 to minute 480. As it can be seen from this diagram, the trend is rising in the predominant minutes. This is justified because the capital investment related to the nth time step is added to the total outlet cost of the $(n-1)$th time step; however, for some time steps, the trend is flat or descending due to variations in the inside air temperature and its exergy flow rate. For the time steps of 400 up to the end, the trend is significantly rising due to two parallel factors of capital investment

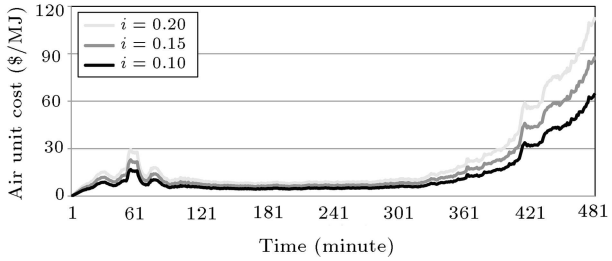

Figure 9. Air unit cost at time steps of $n = 1$ to $n = 480$ for different interest rates.

increase and the air temperature. Therefore, its exergy flow rate is reduced.

Moreover, the air unit cost is highly influenced by the interest rate value as it increases doubly by raising the interest rate from 10% to 20% at the end of the test (Figure 9).

4. Conclusion

This study conducts the energetic, exergetic, and economic simulation of an innovative semi-solar greenhouse structure using MATLAB software and analysis of its performance. This modeling was performed to predict the temperatures in four different area points inside the semi-solar greenhouse based on the crop evapotranspiration influence. In addition, the total exergy destruction values in different heat and mass transfer processes were inspected. In this regard, the greenhouse air unit cost for each time step including the one-minute step was analyzed. Furthermore, the results of the proposed thermodynamic analysis were evaluated using the measured data retrieved from the constructed typical semi-solar greenhouse. The most important conclusions induced from this research are as follows:

- Increasing the temperature of the greenhouse air during the test to 33°C on a cold day illustrates that the greenhouse performance is efficient in absorbing and keeping the solar energy;
- Uncertainty assessment results indicated that the experimental data recorded during the tests were reliable so as to evaluate the accuracy of the thermodynamic modeling;
- According to statistical analysis results, it was proved that the thermal modeling results were consistent with experimental measurements;
- Total exergy destruction associated with convection and radiation processes between the greenhouse cover and other components had the highest value among the other procedures;
- The technique of using a standard type of two-layer glass as a greenhouse cover could reduce the exergy destructions of convection and radiation processes;
- The exergy destruction associated with the condensation of vapor on the inside surface of the greenhouse cover and respiration of the crop were very low and insignificant;
- Considering that the target of this research was to provide suitable environmental conditions for the inside of the greenhouse, the air unit cost was inspected from the first step time to the end;
- Exergoeconomic evaluation illustrated that the air unit cost trend was rising in most minutes;
- The air unit cost was highly influenced by the interest rate value.

Acknowledgments

This study was supported by University of Tabriz, Iran. The authors are grateful for the support provided by this University.

Nomenclature

A	Surface area (m^2)
AIR	Enthalpy transfer by dry air (W)
C	Cost ($)
$\dot{C}$	Cost rate ($/s)
c	Cost of air unit ($/J)
CD	Enthalpy transfer by conduction (W)
CRF	Capital Recovery Factor (–)
CV	Enthalpy transfer by convection (W)
$C_{H_2O,a}$	Water vapor concentration at inside air temperature (kgH_2O/s)
$C_{H_2O,o}$	Water vapor concentration at outside air temperature (kgH_2O/s)
$C_{H_2Os,p}$	Water vapor saturation concentration at plant temperature (kgH_2O/s)
$C_{H_2Os,coi}$	Water vapor saturation concentration at inside cover temperature (kgH_2O/s)
d	Thickness (m)
E	Emission coefficient (–)
$EX_{a,dif}$	Diffusional exergy of inside air (W)
$EX_{a,th}$	Thermal exergy of inside air (W)
EX_d	Exergy destruction (W)
F	View factor (–)
f	Dependency factor for R_{s-H_2O} (–)
f_a	Infiltration factor (–)
H_2O	Enthalpy transfer by vapor (W)
I	Solar radiation (W/m^2)
i	Interest rate (–)

IL	Enthalpy transfer by long wave radiation (W)
IS	Enthalpy transfer by short wave radiation (W)
I_{p-g}	Heat absorbed by canopy (W/m^2)
M_{air}	Molar mass of dry air (kg/mol)
$M_{\text{H}_2\text{O}}$	Molar mass of water (kg/mol)
n	Mass flow of species (mol)
op_{vhr}	Option ventilation heat recovery (–)
P	Pressure (Pa)
$P_{\text{H}_2\text{O}s,p}$	Saturation vapor pressure for plant (N/m^2)
$P_{\text{H}_2\text{O},a}$	Vapor pressure of indoor air (N/m^2)
p_i	Partial pressure (Pa)
Q	Heat transfer (W)
R	Resistance (s/m)
R_a	Gas constant of dry air (J/(K.mol))
R_v	Gas constant of H_2O vapour (J/(K.mol))
r_w	Water evaporation heat (j/kg)
T	Temperature (K)
t	Time (s)
V	Volume (m^3)
Z_k	Capital investment ($)
$\dot{Z}_k$	Capital investment rate ($/s)
α	Convection heat transfer coefficient (W/(m^2 K))
ρ	Density (kg/m^3)
λ	Conduction heat transfer coefficient (W/mK)
η_{rd}	Short wave radiation absorption coefficient (–)
ϕ	Volume flow air (m^3/s)
ϕ_m	Mass flow rate (kg/s)
v	Wind velocity (m/s)
β_{g-Is}	Shortwave reflection coefficient by ground (–)
$\Delta_{pp-\text{H}_2\text{O}m}$	Saturation deficit of plant (mbar)
η_{vhr}	Efficiency of ventilation heat recovery (–)
ω	Absolute humidity (kg H_2O vapor/kg dry air)
Φ_r	Maintenance factor (–)

Subscripts

a	Inside air
air	Air
coi	Inside cover
coo	Outside cover
De	Destruction
dg	Deep ground
dif	Diffusional
e	Environment
g	Inside ground
H_2O	Water
in	Inlet
leak	Leakage
m	Mass
nw	North wall
nwi	Inside north wall
nwo	Outside north wall
o	Outdoor air
p	Plant
q	Heat
rd	Radiation
sc	Screen
sk	Sky
th	Thermal
out	Outlet
vhr	Ventilation heat recovery
w	Work

References

1. Kıyan, M. Bingol, E. Melikog, M., et al. "Modelling and simulation of a hybrid solar heating system for greenhouse applications using MATLAB/SIMULINK", *Energy Conversion and Management*, **72**, pp. 147–155 (2013).
2. Gorjian, S., Calise, F., Kant, K., et al. "A review on opportunities for implementation of solar energy technologies in agricultural greenhouses", *Journal of Cleaner Production*, **285**, p. 124807 (2020).
3. Kondili, E. and Kaldellis, J. "Optimal design of geothermal-solar greenhouses for the minimisation of fossil fuel consumption", *Applied Thermal Engineering*, **26**(8–9), pp. 905–915 (2006).
4. Li, Z., Ehyaei, M.A., Ahmadi, A., et al. "Energy, exergy and economic analyses of new coal-fired cogeneration hybrid plant with wind energy resource", *Journal of Cleaner Production*, **269**, p. 122331 (2020).
5. Li, Z., Khanmohammadi, S., Khanmohammadi, S., et al. "3-E analysis and optimization of an organic rankine flash cycle integrated with a PEM fuel cell and geothermal", *International Journal of Hydrogen Energy*, **45**(3), pp. 2168–2185 (2020).

6. Li, Z., Khanmohammadi, S., Khanmohammadi, S., et al. "Multi-objective energy and exergy optimization of different configurations of hybrid earth-air heat exchanger and building integrated photovoltaic/thermal system", *Energy Conversion and Management*, **195**, pp. 1098–1110 (2019).
7. Ziapour, B.M. and Hashtroudi, A. "Performance study of an enhanced solar greenhouse combined with the phase change material using genetic algorithm optimization method", *Applied Thermal Engineering*, **110**, pp. 253–264 (2017).
8. Sajid, M.U. and Bicer, Y. "Comparative life cycle cost analysis of various solar energy-based integrated systems for self-sufficient greenhouses", *Sustainable Production and Consumption*, **27**, pp. 141–156 (2021).
9. Attar, I. and Farhat, A. "Efficiency evaluation of a solar water heating system applied to the greenhouse climate", *Solar Energy*, **119**, pp. 212–224 (2015).
10. Zhang, J., Wang, J., Guo, S., et al. "Study on heat transfer characteristics of straw block wall in solar greenhouse", *Energy and Buildings*, **139**, pp. 91–100 (2017).
11. Bazgaou, A., Fatnassi, H., Bouharroud, R., et al. "Performance assessment of combining rock-bed thermal energy storage and water filled passive solar sleeves for heating Canarian greenhouse", *Solar Energy*, **198**, pp. 8–24 (2020).
12. Joudi, K.A. and Farhan, A.A. "Greenhouse heating by solar air heaters on the roof", *Renewable Energy*, **72**, pp. 406–414 (2014).
13. Vadiee, A. and Martin, V. "Energy analysis and thermoeconomic assessment of the closed greenhouse-The largest commercial solar building", *Applied Energy*, **102**, pp. 1256–1266 (2013).
14. Zhang, G., Ding, X., Li, T., et al. "Dynamic energy balance model of a glass greenhouse: An experimental validation and solar energy analysis", *Energy*, **198**, p. 117281 (2020).
15. Chen, C., Yu, N., Yang, F., et al. "Theoretical and experimental study on selection of physical dimensions of passive solar greenhouses for enhanced energy performance", *Solar Energy*, **191**, pp. 46–56 (2019).
16. Zhang, X., Lv, J., Dawuda, M.M., et al. "Innovative passive heat-storage walls improve thermal performance and energy efficiency in Chinese solar greenhouses for non-arable lands", *Solar Energy*, **190**, pp. 561–575 (2019).
17. Mahdavi, S., Sarhaddi, F., and Hedayatizadeh, M. "Energy/exergy based-evaluation of heating/cooling potential of PV/T and earth-air heat exchanger integration into a solar greenhouse", *Applied Thermal Engineering*, **149**, pp. 996–1007 (2019).
18. Chen, W., Liu, W., and Liu, B. "Numerical and experimental analysis of heat and moisture content transfer in a lean-to greenhouse", *Energy and Buildings*, **38**(2), pp. 99–104 (2006).
19. Yildizhan, H. and Taki, M. "Assessment of tomato production process by cumulative exergy consumption approach in greenhouse and open field conditions: Case study of Turkey", *Energy*, **156**, pp. 401–408 (2018).
20. Sethi, V. and Sharma, S. "Experimental and economic study of a greenhouse thermal control system using aquifer water", *Energy Conversion and Management*, **48**(1), pp. 306–319 (2017).
21. Iran Meteorological organization. http://eamo.ir/Stats-and-Infos/Yearly.aspx
22. Bell, S. "A beginner's guide to uncertainty of measurement", *Measurement Good Practice Guide*, **11**, p. 1 (1999).
23. Zarifneshat, S., Rohani, A., Ghassemzadeh, H.R., et al. "Predictions of apple bruise volume using artificial neural network", *Computers and Electronics in Agriculture*, **82**, pp. 75–86 (2012).
24. Glover, M. and Reichert, G. "Convective gas-flow inhibitors", Google Patents (1994).
25. Jester, T.C., *Twentieth-Century Building Materials: History and Conservation*, Getty Publications (2014).
26. Van Ooteghem, R., *Optimal Control Design for a Solar Greenhouse, Systems and Control*, Wageningen: Wageningen University (2007).
27. Van Straten, G., Van Willigenburg, G., Van Henten, E., et al., *Optimal Control of Greenhouse Cultivation*, CRC press (2010).
28. Bot, G.P. Greenhouse Climate: from Physical Processes to a Dynamic Model, Landbouwhogeschool te Wageningen (1993).
29. De Jong, T., *Natural Ventilation of Large Multi-Span Greenhouses*, De Jong (1990).
30. Moran, M.J., Shapiro, H.N., Boettner, D.D., et al., *Fundamentals of Engineering Thermodynamics*, John Wiley & Sons (2010).
31. Bronchart, F., De Paepe, M., Dewulf, J., et al. "Thermodynamics of greenhouse systems for the northern latitudes: Analysis, evaluation and prospects for primary energy saving", *Journal of Environmental Management*, **119**, pp. 121–133 (2013).
32. Kenneth Wark, D.E.R., *Thermodynamics McGraw-Hill Series in Mechanical Engineering*, ISBN-13: 978-0071168533, p. 954 (1999).
33. Bejan, A., Tsatsaronis, G., Moran, M.J., et al., *Thermal Design and Optimization*, John Wiley & Sons (1996).
34. Lambe, D.P., Adams, S.A., and Paparozzi, E.T. "Estimating construction costs for a low-cost Quonset-style greenhouse", Agronomy & Horticulture Faculty Publications, University of Nebraska, **752**, pp. 1–8 (2012).
35. Indicators, E. "Marshall&Swift equipment cost index", *Chemical Engineering*, **72**, pp. 14–15 (2011).

36. Ahmadi, P. and Dincer, I. "Thermodynamic and exergoenvironmental analyses, and multi-objective optimization of a gas turbine power plant", *Applied Thermal Engineering*, **31**(14–15), pp. 2529–2540 (2011).

37. Gupta, A. and Tiwari, G. "Computer model and its validation for prediction of storage effect of water mass in a greenhouse: a transient analysis", *Energy Conversion and Management*, **43**(18), pp. 2625–2640 (2002).

38. Boulard, T. and Baille, A. "Analysis of thermal performance of a greenhouse as a solar collector", *Energy in Agriculture*, **6**(1), pp. 17–26 (1987).

39. Abdel-Ghany, A. and Al-Helal, I. "Solar energy utilization by a greenhouse: General relations", *Renewable Energy*, **36**(1), pp. 189–196 (2011).

40. Abdel-Ghany, A.M. and Kozai, T. "Dynamic modeling of the environment in a naturally ventilated, fog-cooled greenhouse", *Renewable Energy*, **31**(10), pp. 1521–1539 (2006).

41. Abdel-Ghany, A.M. "Solar energy conversions in the greenhouses", *Sustainable Cities and Society*, **1**(4), pp. 219–226 (2011).

42. Jain, D. and Tiwari, G. "Modeling and optimal design of ground air collector for heating in controlled environment greenhouse", *Energy Conversion and Management*, **44**(8), pp. 1357–1372 (2003).

43. Singh, R. and Tiwari, G. "Energy conservation in the greenhouse system: A steady state analysis", *Energy*, **35**(6), pp. 2367–2373 (2010).

44. Mashonjowa, E., Ronsse, F., Milford, J.R., et al. "Modelling the thermal performance of a naturally ventilated greenhouse in Zimbabwe using a dynamic greenhouse climate model", *Solar Energy*, **91**, pp. 381–393 (2013).

45. Sharma, P., Tiwari, G., and Sorayan, V. "Temperature distribution in different zones of the micro-climate of a greenhouse: a dynamic model", *Energy Conversion and Management*, **40**(3), pp. 335–348 (1999).

46. Du, J., Bansal, P., and Huang, B. "Simulation model of a greenhouse with a heat-pipe heating system", *Applied Energy*, **93**, pp. 268–276 (2012).

Biographies

Behzad Mohammadi is a professional Mechanical Engineer with over 9 years of progressive experience in oil and gas industry and comprehensive knowledge in gas turbine maintenance. His education background in Mechanical Engineering and deep process engineering experiences have been proven to be effective in performing duties as an Mechanical Engineer. The determination, analytical skill, and attention to detail that he possesses are also helping in maximizing his performance so far. His intellectual curiosity about engineering and his passion for asking questions are what have led him to pursue PhD in Mechanical Engineering in conjunction with industrial work.

Seyed Faramarz Ranjbar has conducted many researches on energy, exergy and environmental analysis of systems and optimization. He is a Professor at the Mechanical Engineering Department at University of Tabriz. He has 48 ISI article papers and has received many awards for his extensive scientific services including the use of steam turbines in turbochargers of marine diesel engines and the design of a high-performance practical Stirling engine with water vapor.

Yahya Ajabshirchi is interested in the subject of solar greenhouse and has offered a lot of article papers in this field. He is a Professor at Agricultural Engineering Department at University of Tabriz. Although he is a Professor at the Faculty of Agriculture, he has authored a book on internal combustion engines. He has supervised many doctoral and Master's theses and is now retired after years of scientific service.